CHAPTER 4

RESULTS AND DISCUSSIONS

4.1 WELD MACROSTRUCTURE

The macro section of the weldments of DSS and SDSS joints are shown in Figure 4.1. The weldment is divided into weld cap, weld root and heat affected zone (HAZ).

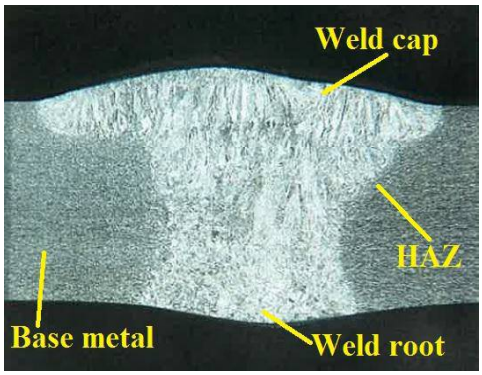

a) DSS weldments

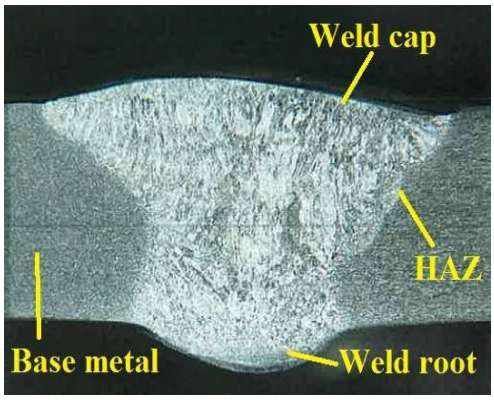

b) SDSS weldments

Figure 4.1: Macrostructure of welded joints

4.2 WELD MICROSTRUCTURE

The typical microstructures of weld cap and weld root is shown in Figure 4.2. The weld root region has been re-heated during subsequent weld passes. Hence, intragranular primary austenite and acicular type secondary austenite are formed at root. The reheating of weld root region is the reason for formation of secondary austenite and sigma phases [153]. The amount of austenite formed is higher in root region than that in weld cap. The weld cap region comprises of grain boundary austenite, intragranular and Widmänstten austenite formed in a ferrite matrix. The coarse ferrite grains are observed in weld cap region.

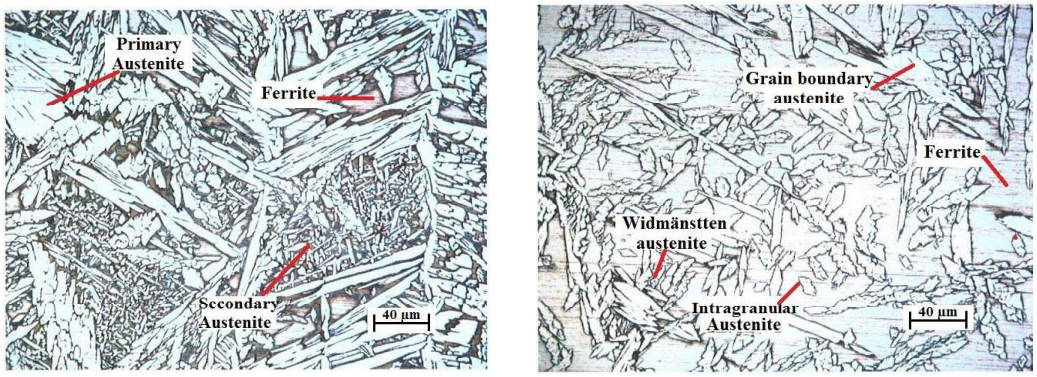

a) Weld root microstructure b) Weld cap microstructure

Figure 4.2: Typical weld microstructures

When high heat input is employed (i.e. slower cooling rate), large grain size and higher contents of austenite are obsereved. When low heat input is applied (i.e. higher cooling rate), finer grains are formed with lower austenite content as shown in Figure 4.3.

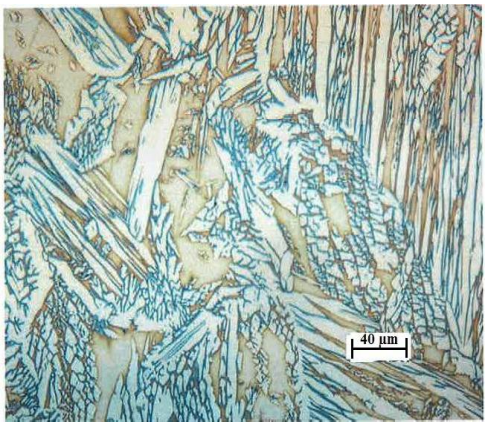

a) Weld metal cap at high heat input

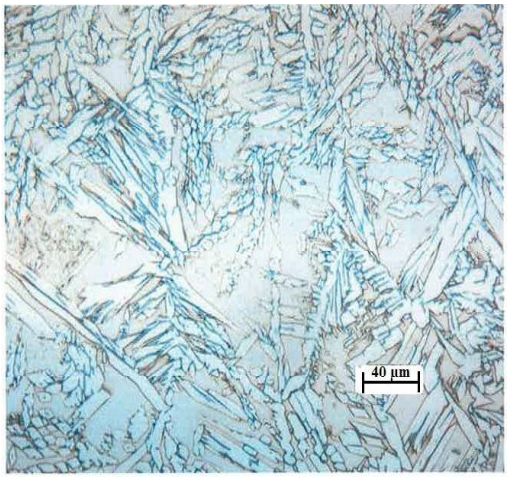

b) Weld metal cap at low heat input

Figure 4.3: Microstructural variation with heat input

The HAZ microstructures are shown in Figure 4.4. It depends on highest temperature attained by this region. Generally, this temperature is below solidus temperature point. In this region, an increase in grain size was obsereved due to recrystallization, particularly in ferrite.

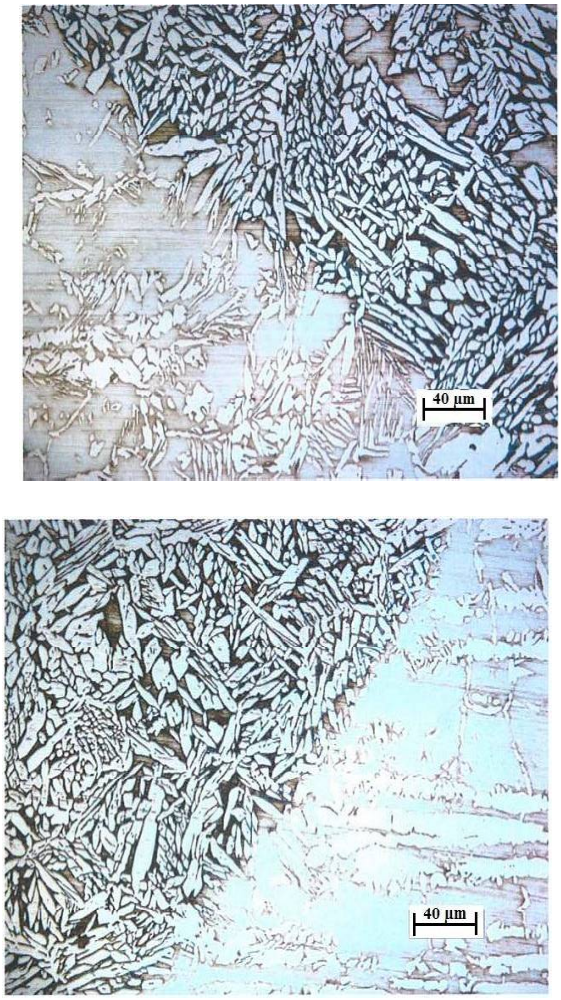

Figure 4.4: Heat affected zones

The ferrite contents of welded specimens are studied for DSS and SDSS materials with varying PREN, heat input, interpass temperature and shielding gas

composition. Effect of heat input on Ferrite Content (%) of DSS weldments with varying PREN are tabulated in Table 4.1.

Table 4.1- Effect of heat input on Ferrite Content (%) of DSS weldments

Specimen	Heat Input (kJ/mm)	Cap	Root	HAZ-Cap	HAZ-Root
DSS- Low PREN	1.05	54 ± 3	38 ± 4	54 ± 5	48 ± 3
	1.10	46 ± 2	43 ± 5	52 ± 3	43 ± 5
	1.15	39 ± 4	36 ± 3	55 ± 2	51 ± 3
	1.20	35 ± 3	34 ± 3	50 ± 1	48 ± 4
DSS- High PREN	1.0	45 ± 2	39 ± 2	51 ± 1	50 ± 2
	1.05	55 ± 2	35 ± 5	65 ± 4	60 ± 4
	1.1	44 ± 1	42 ± 2	50 ± 2	44 ± 4
	1.15	38 ± 3	35 ± 3	44 ± 1	43 ± 3

It has been observed that weld cap contains more ferrite than root region for both fusion zone and heat affected zone. It can be also observed that ferrite volume fraction in HAZ was higher than that of weld region.

At the same time, it can be seen that the amount of austenite formed in high PREN grade is higher than that of low PREN grade. This is because of enrichment of autenite stablizers in high PREN grade.

The bar charts shown in Figures 4.5 (a) and (b) represent ferrite content values with different Heat input for DSS material.

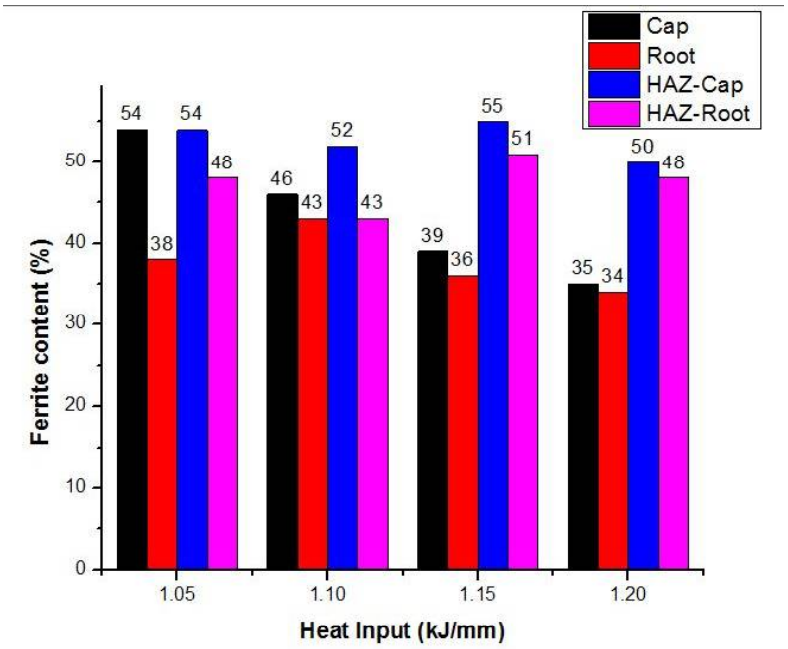

a) DSS – Low PREN

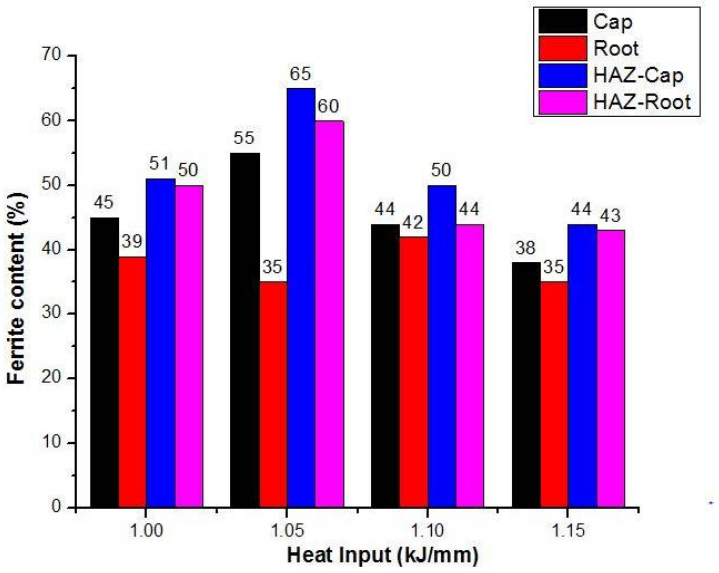

b) DSS – High PREN

Figure 4.5: Bar charts for ferrite content measurements

Effect of heat input on Ferrite Content (%) of SDSS weldments with varying PREN are tabulated in Table 4.2.

Table 4.2- Effect of heat input on Ferrite Content (%) of SDSS weldments

Specimen	Heat Input (kJ/mm)	Cap	Root	HAZ-Cap	HAZ-Root
SDSS-Low PREN	0.95	56 ± 2	39 ± 5	42 ± 3	39 ± 1
	1.05	48 ± 1	46 ± 3	49 ± 2	48 ± 2
	1.15	48 ± 3	43 ± 4	49 ± 2	47 ± 1
	1.25	46 ± 4	38 ± 3	48 ± 3	45 ± 1
	0.75	64 ± 4	46 ± 5	61 ± 3	56 ± 3
	1.0	58 ± 3	49 ± 2	56 ± 1	55 ± 3

SDSS-High PREN	1.1	55 ± 3	51 ± 3	51 ± 2	48 ± 3
	1.2	52 ± 4	45 ± 4	48 ± 2	43 ± 3

We observed similar trend in SDSS material like DSS that more ferrite than root region.

The bar charts shown in Figure 4.6 (a) and (b) represent ferrite content values with different Heat input for SDSS material

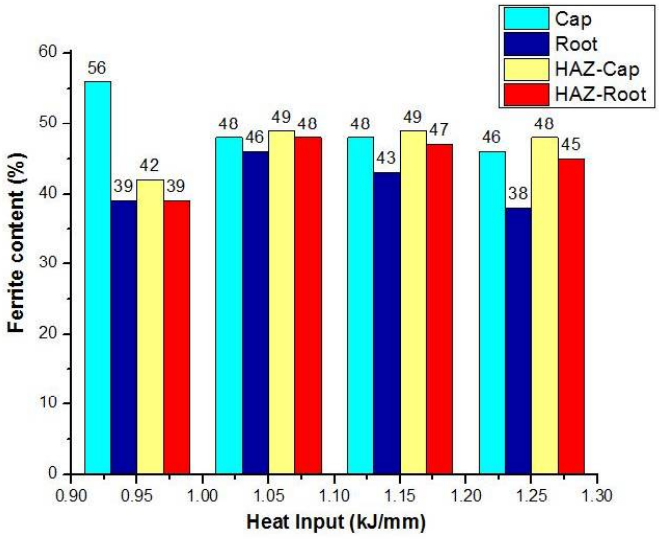

a) SDSS- Low PREN

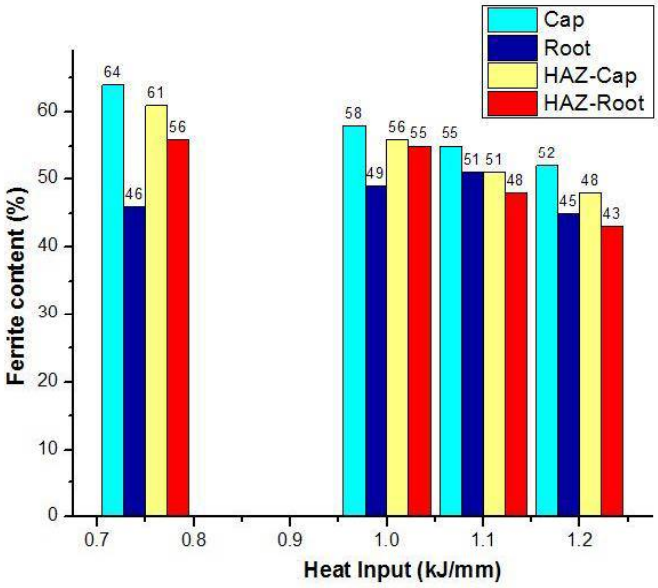

b) SDSS – High PREN

Figure 4.6: Bar charts for ferrite content measurements

Effect of shielding/purging gas and inter-pass temperature on Ferrite content (%) measurements of DSS weldments are tabulated in Table 4.3.

Table 4.3- Effect of shielding/purging gas and inter-pass temperature on Ferrite content (%) measurements of DSS weldments

Exp. no.	Cap	Root	HAZ-Cap	HAZ-Root
1 (Ar+2%N_2, 120 ^{O}C)	54 ± 2	38 ± 4	54 ± 5	48 ± 2
2 (Ar+5%N_2, 120 ^{O}C)	51 ± 3	37 ± 2	50 ± 3	46 ± 1
3 (Ar+2%N_2, 160 ^{O}C)	49 ± 4	34 ± 5	48 ± 3	46 ± 2
4 (Ar+2%N_2, 160 ^{O}C)	68 ± 1	46 ± 4	61 ± 4	43 ± 3

With addition of nitrogen in shielding/purging gas [i.e. Ar+5%N], the ferrite content is found to decrease as nitrogen is an austenite stabilizer. Thus, proper elemental partitioning and more balanced microstructure is achieved [163]. An increase in interpass tempearature leads to slight decrease in ferrite content in weld region and HAZ. Intermetallics phases are also formed in weld zone due to continued exposure to sensitive high temperatures where diffusion of ferrite into sigma phase and secondary austenite is noticed.

The bar chart shown in Figure- 4.7 represents ferrite content of DSS weldment with different shielding / purging gas and inter-pass temperature.

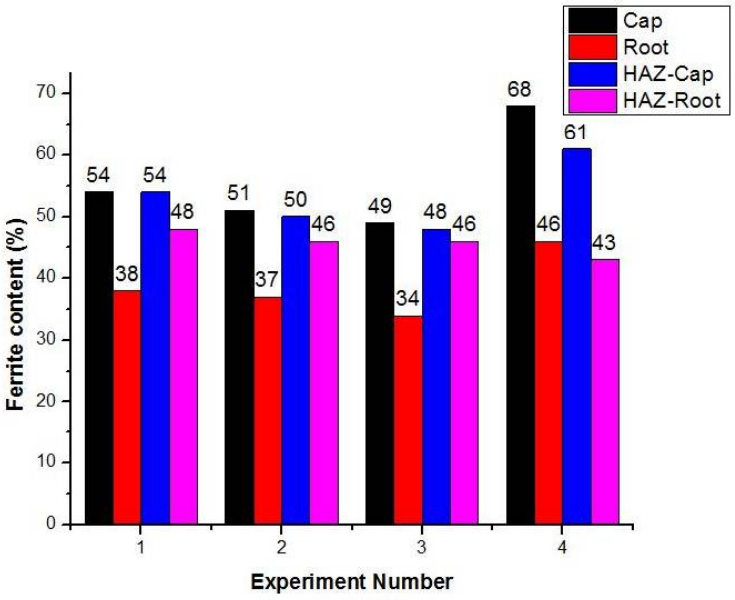

Figure 4.7: Bar charts for ferrite content measurements - DSS

Effect of shielding/purging gas and inter-pass temperature on Ferrite content (%) measurements of SDSS weldments are tabulated in Table 4.4.

Table 4.4- Effect of shielding/purging gas and inter-pass temperature on Ferrite content (%) measurements of SDSS weldments

Exp. no.	Cap	Root	HAZ-Cap	HAZ-Root
1 ($Ar+2\%N_2$, 120 ^{O}C)	56 ± 3	39 ± 4	42 ± 2	39 ± 3
2 ($Ar+5\%N_2$, 120 ^{O}C)	51 ± 2	37 ± 5	41 ± 1	37 ± 3
3 ($Ar+2\%N_2$, 160 ^{O}C)	49 ± 4	34 ± 3	41 ± 1	39 ± 2
4 ($Ar+2\%N_2$, 160 ^{O}C)	70 ± 3	46 ± 4	64 ± 2	44 ± 4

It has been noticed that ferrite percentage are lowered when Nitrogen content are increased in shielding/purging gas. Similarly, increasing inter-pass temperature reduces ferrite percentage. Higher intermetallics phases are observed in SDSS than DSS material in weld zone due to continued exposure to sensitive high temperatures.

The bar chart shown in Figure- 4.8 represents ferrite content of DSS weldment with different shielding / purging gas and inter-pass temperature.

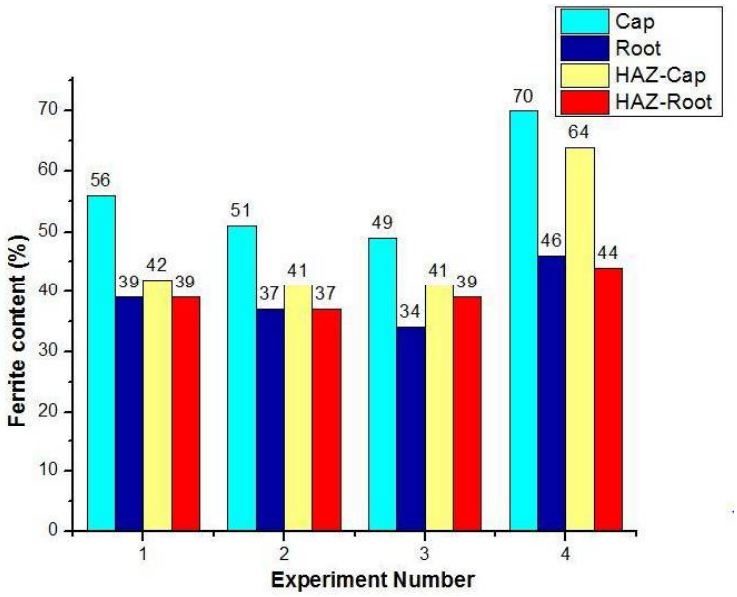

Figure 4.8: Bar charts for ferrite content measurements - SDSS

4.3 MECHANICAL TEST RESULTS

The mechanical properties of different welded joints as measured experimentally for different heat input and different composition of shielding/purging gas composition. Effect of Heat Input on Mechanical Properties of the DSS and SDSS weld joints are tabulated in Tables 4.5.

Table 4.5- Effect of Heat Input on Mechanical Properties of the weld joints

Exp. No.	Specimen	Heat Input (kJ/mm)	Tensile Strength (MPa)	Impact Toughness at - 46 °C (J)	Hardness (VHN)
DSS					
1	DSS- Low PREN	1.05	795	168	266
2		1.10	780	140	264
3		1.15	767	123	259

4		1.20	755	85	255
5	DSS- High PREN	1.0	805	115	275
6		1.05	802	104	270
7		1.1	785	97	266
8		1.15	777	94	261
SDSS					
1	SDSS- Low PREN	0.95	862	140	319
2		1.05	844	130	312
3		1.15	827	126	298
4		1.25	805	107	288
5	SDSS- High PREN	0.75	896	90	326
6		1.0	880	81	320
7		1.1	855	72	315
8		1.2	835	64	302

From the results of mechanical tests on DSS welded joints, it is observed that tensile strength, impact strength and hardness of the joints decreases with increasing heat input during welding for low PREN grade as well as for high PREN grade.

The comparative bar charts representing the effect of heat input on the mechanical properties for different weld joints are shown in Figures 4.9 (a) to (d)

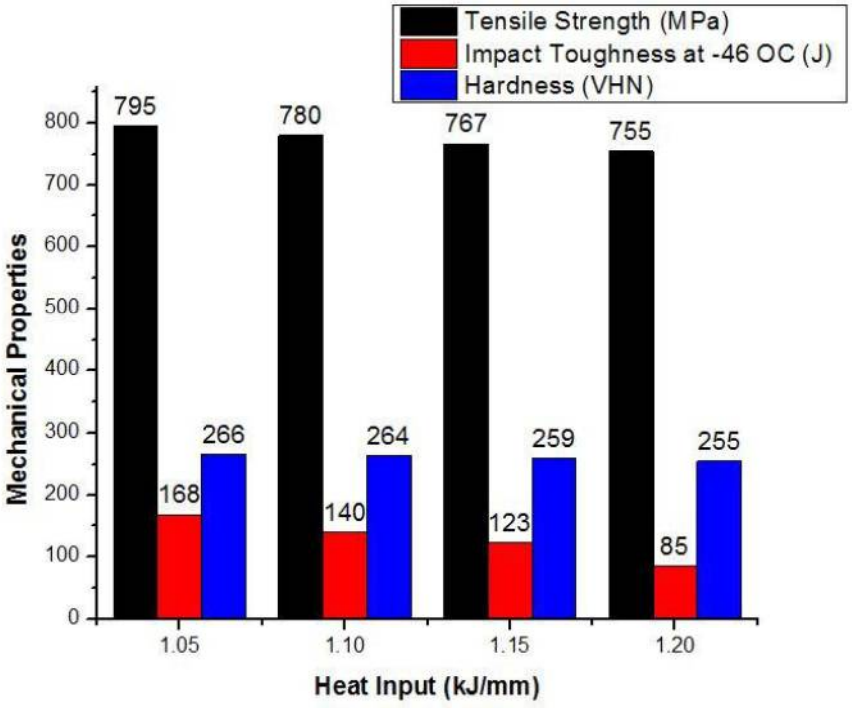

a) DSS- Low PREN

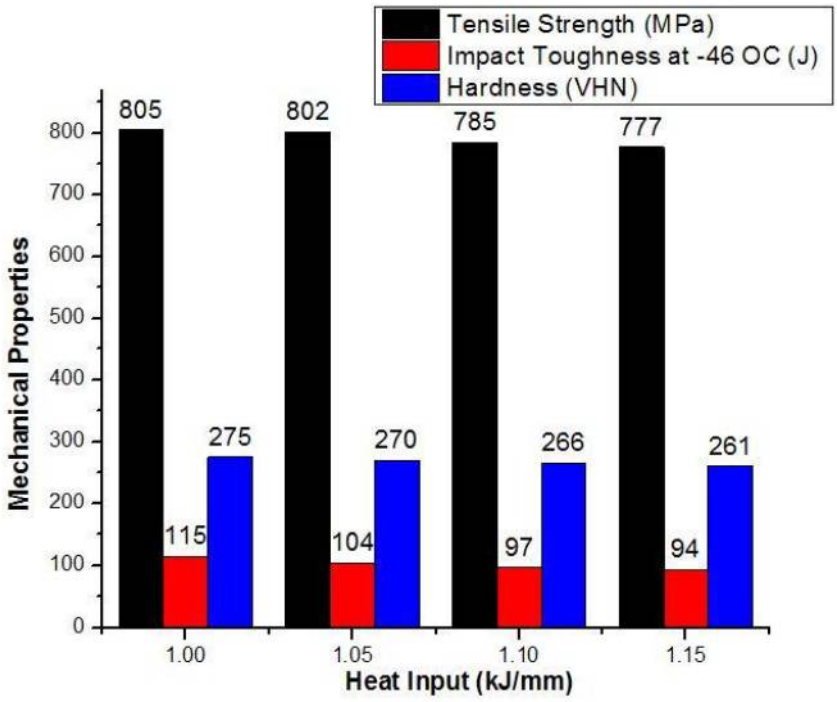

b) DSS – High PREN

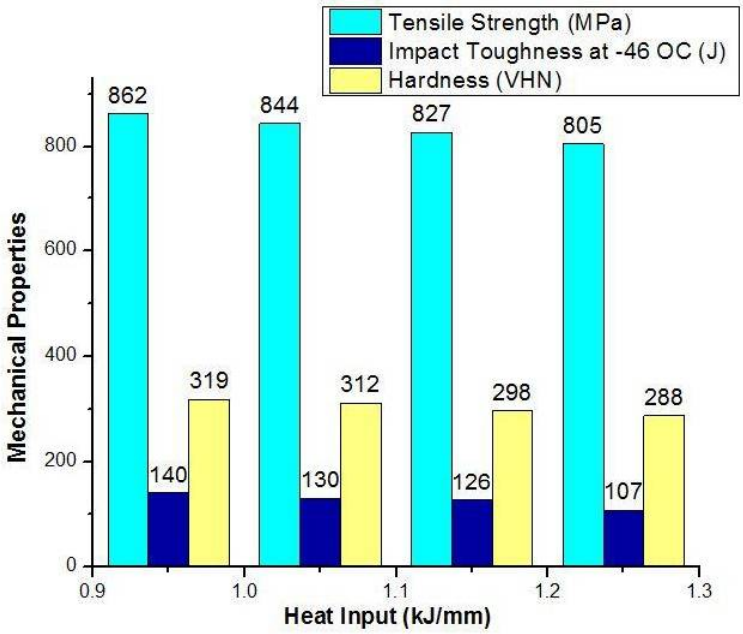

c) SDSS – Low PREN

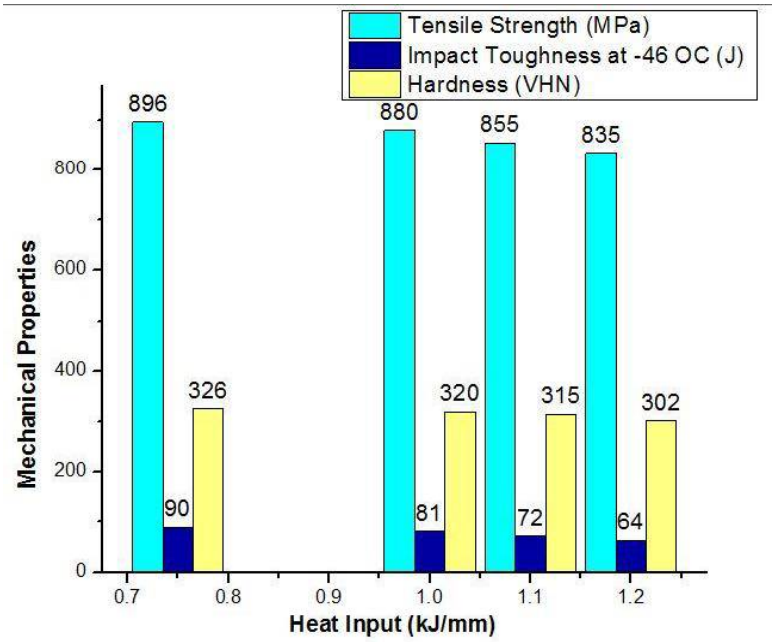

d) SDSS – High PREN

Figure 4.9: Effect of Heat input on Mechanical test results

Effect of shielding/purging gas composition and inter-pass temperature on mechanical properties of DSS and SDSS welds are tabulated in Table 4.6.

Table 4.6- Effect of shielding/purging gas and inter-pass temperature on mechanical properties of the weld joint

Experiment No.	Heat Input (kJ/mm)	Tensile Strength (MPa)	Hardness (VHN)	Impact Toughness at - 46 ^{O}C (J)
DSS				
1 (Ar+2%N_2, 120 ^{O}C)	1.05	805	275	112
2 (Ar+5%N_2, 120 ^{O}C)	1.05	820	281	131
3 (Ar+2%N_2, 160 ^{O}C)	1.05	818	277	135
4 (Ar+2%N_2, 160 ^{O}C)	1.05	784	290	86
SDSS				
1 (Ar+2%N_2, 120 ^{O}C)	1.05	880	312	130
2 (Ar+5%N_2, 120 ^{O}C)	1.05	895	322	146
3 (Ar+2%N_2, 160 ^{O}C)	1.05	888	317	143
4 (Ar+2%N_2, 160 ^{O}C)	1.05	868	319	104

It has been observed that increasing Nitrogen content in shielding gas composition increases mechanical properties for both DSS and SDSS materials.

The comparative bar charts representing the effect of shielding / purging gas on mechanical properties are shown in Figure 4.10 (a) and (b).

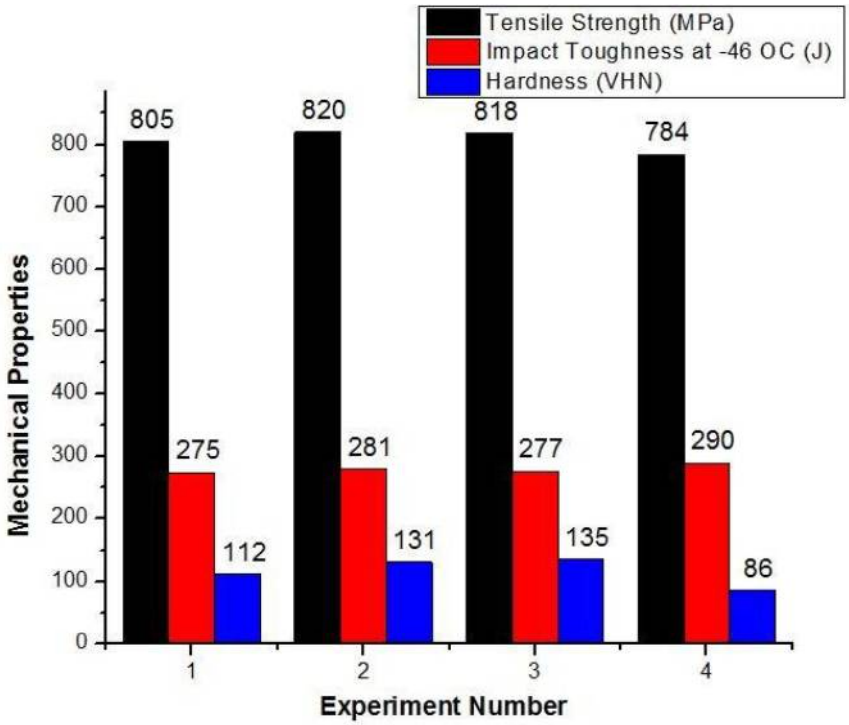

a) Bar Chart for Mechanical Test - DSS

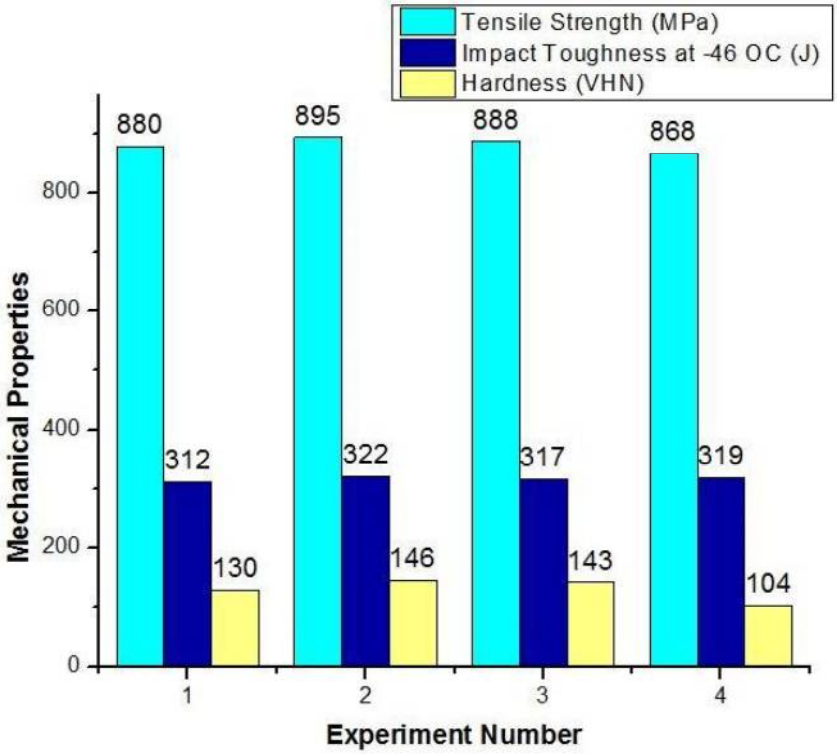

b) Bar chart for Mechanical Test – SDSS

Figure 4.10: Mechanical test results

4.3.1 Tensile Strength

Tensile test results are tabulated in Table 4.5 and 4.6. All the test samples exhibited excellent tensile strength. Both DSS and SDSS weldments exhibited higher tensile strength value than the base metal. All the test samples were fractured outside the weld region. The weld strength is found to be 5-10 % more as compared to base material. As the selected filler wire strength is higher than the base metal, it is evident that the weld metal strength is higher than the base metal and noted that the fracture occurred well away from the weld metal. The highest strength obtained is 820 MPa and 896 MPa for DSS and SDSS respectively. The fractograph is shown in Figure 4.11 (a) and (b)., which indicates ductile mode of fracture where micro/macro void coalescence (i.e. dimples) is visible.

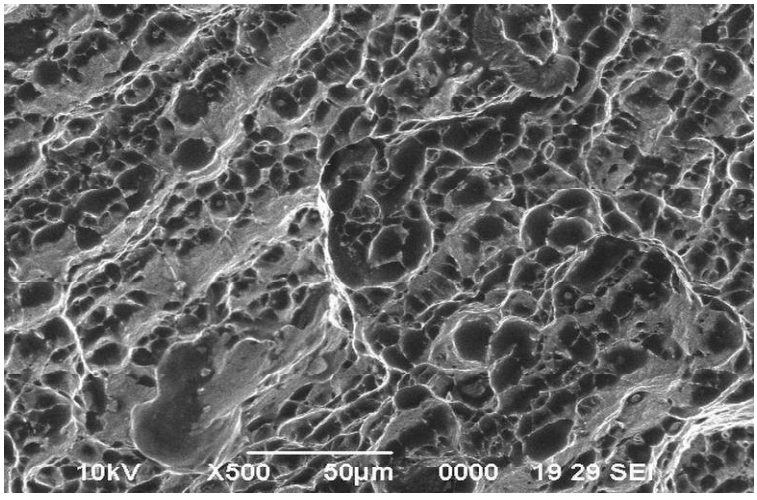

a) DSS weldments

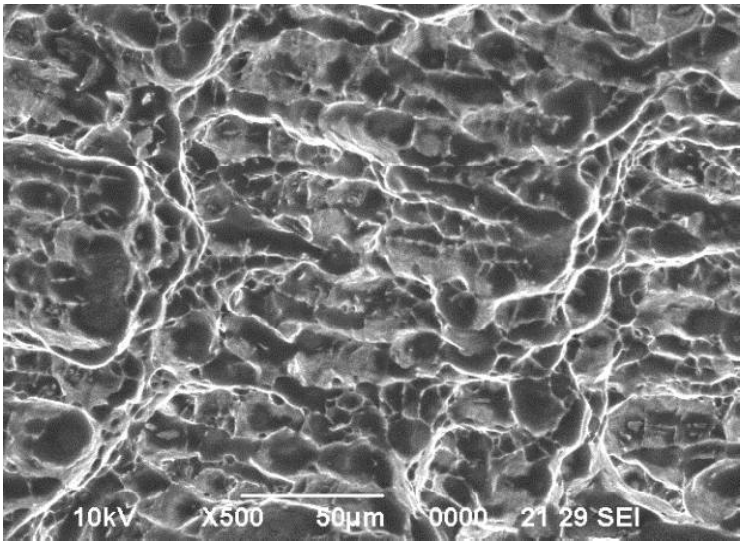

b) SDSS weldments

Figure 4.11: SEM images of fractured surfaces in tensile tests

It is observed that low heat input gives higher tensile strength as compared to high heat inputs. This is due to higher cooling rates induced in low heat input welding which results in finer grains. The other reason is at low heat input [high cooling rate] more ferrite is formed which is stronger between the two phases of DSS, thus improved strength of the weldments [3]. The variation of tensile strength with heat input is shown in Figure 4.12.

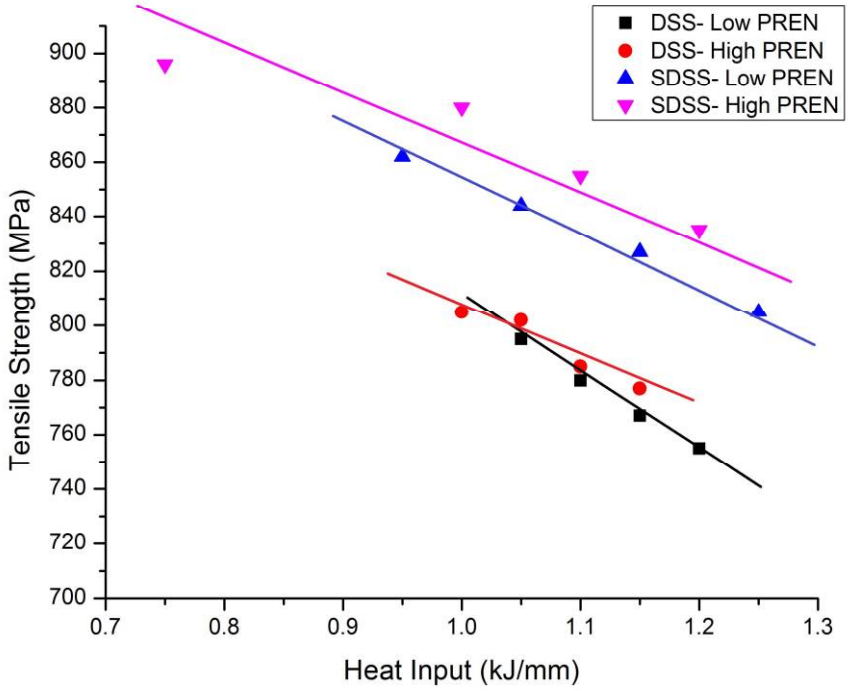

Figure 4.12: Variation of tensile strength with heat input

The effect of shielding gas and purging gas on mechanical properties readings as given in Table 4.6 is analyzed. For both DSS and SDSS welds, it is found that increase in Nitrogen content in shielding and purging gas had a positive effect on tensile properties of weldments. Nitrogen being an austenite stabilizer, affects the weld microstructure. It dissolves mostly in austenite and gives solution-strengthening effect especially to austenite phase. Hence, there is a slight increase in strength of the weldments [164]. On the other hand, increase in interpass temperature results in a decrease in tensile strength. This is due to high temperature, which leads to coarsening of grains and loss of phase balance.

4.3.2 Hardness

The results of hardness measurements taken on Vickers hardness machine which are tabulated in Table 4.5 and Table 4.6 are analyzed. The hardness values of weld metal are found to be higher than the base materials. The variation of hardness with heat input is analyzed as shown in Figure 4.13.

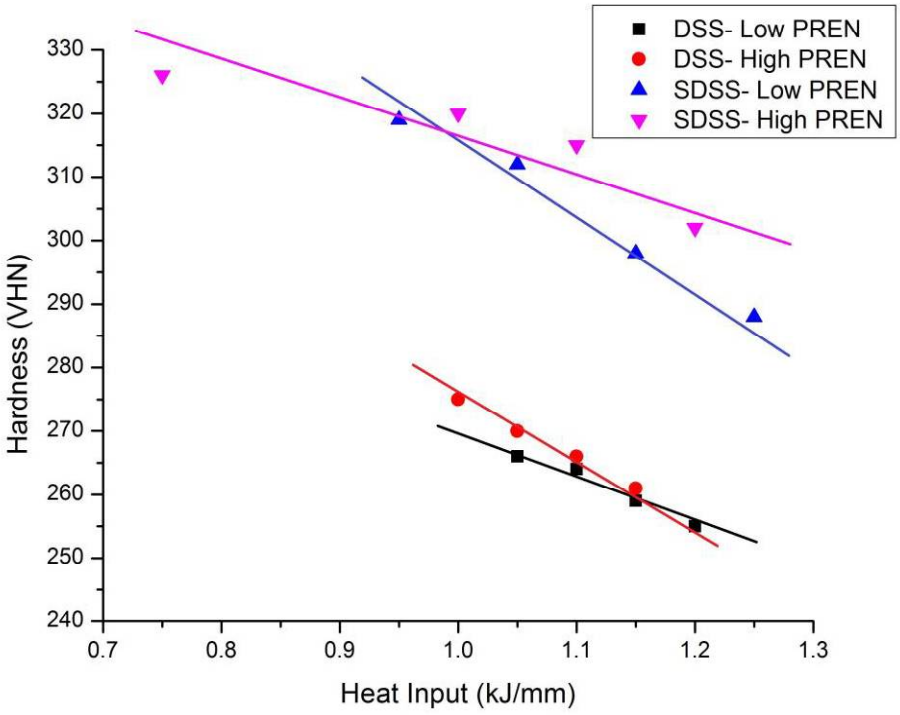

Figure 4.13: Variation of hardness with heat input

It is observed that with low heat input (i.e. higher cooling rate) grain refinement took place, which resulted in high hardness values. Similarly, it is found that weld region exhibited higher hardness than HAZ due to refining of grains. Figure 4.14 (a) and (b). shows hardness variation along the length of the joint.

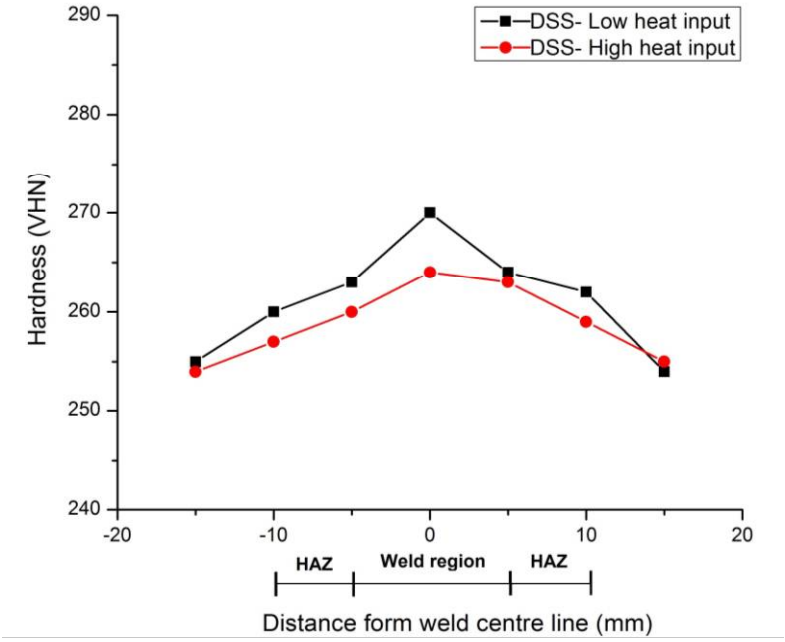

a)DSS weldments

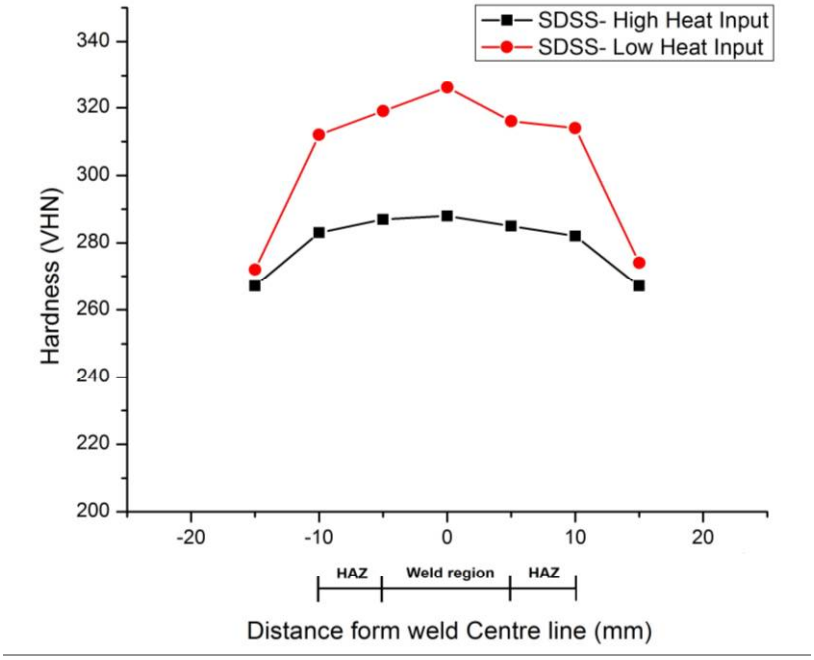

b) SDSS weldments

Figure 4.14: Hardness measurements along transverse section

The hardness values are also measured along the thickness, i.e. below weld cap, weld center and just above weld root. There is a difference between hardness values at each region. A typical distribution of hardness along the thickness of the weldments is shown in Figure 4.15.

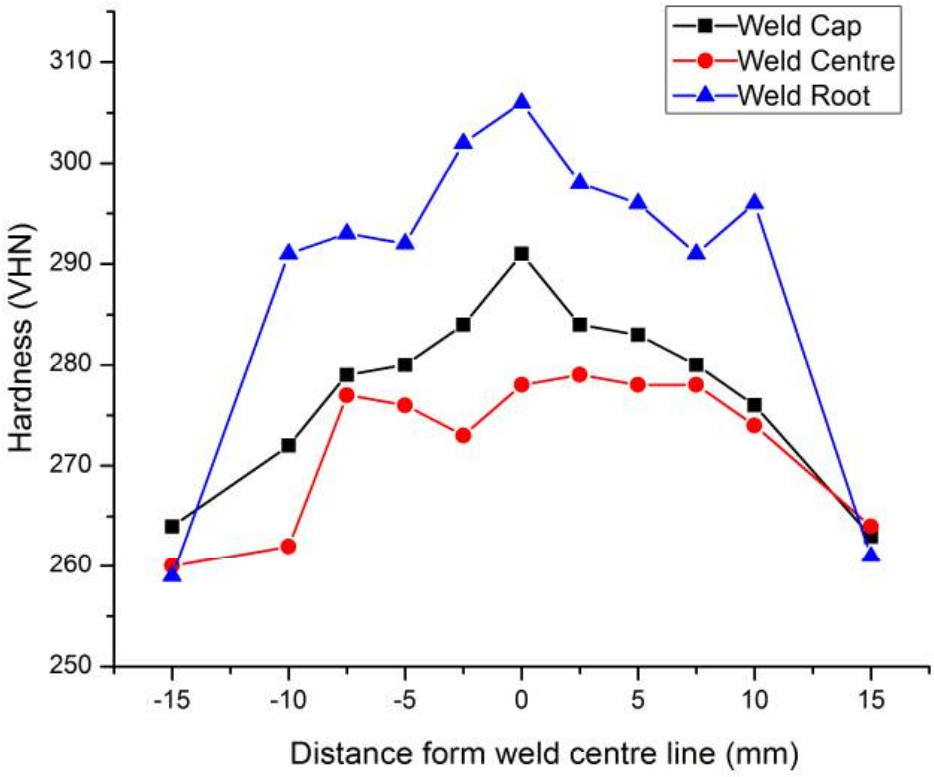

Figure 4.15: Typical hardness distribution in weld region

The weld root region exhibited higher hardness values due to continuous heating and grain refinement. The presence of brittle intermetallic phases could be another reason behind increase in hardness at weld root [159]. Weld center has lower hardness than weld cap region. The weld cap hardness was slightly lower than

root but higher than weld center because of immediate contact of weld cap with air, which facilitates faster cooling thereby increases hardness value.

There is a slight increase of hardness in DSS and SDSS weldments when high nitrogen content gas is used as shielding and purging gas owing to hardening of austenite phase. An increase in interpass temperature promotes increase of hardness value in the weldments. This is due to formation of hard and brittle intermetallic phases, which causes embrittlement.

4.3.3 Impact Toughness

Impact toughness of duplex stainless steel welds depends on many factors such as grain size, austenite reformed after cooling and intermetallic phases precipitation. The effect of heat input on impact toughness of weld metal is shown in Figure 4.16.

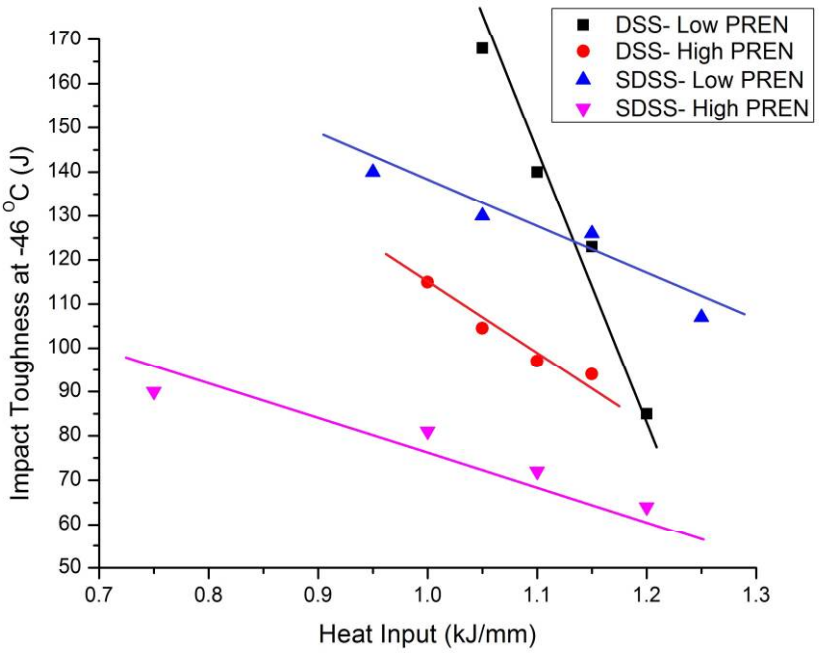

Figure 4.16: Variation of impact toughness (at -46 ^{O}C) with heat input

It is observed that high heat input leads to reduction in toughness of the weld joints. This is because of coarsening of grains at high heat input as compared to fine microstructure at low heat input. Though, high austenite content is obtained with high heat input, there is a precipitation of intermetallic phases (i.e. sigma phase and secondary austenite) which lead to loss of impact toughness. This observation is in accordance with the literature [66, 156].

SDSS base materials have higher toughness values due to higher content of alloying elements. Although, alloying elements such as Cr and Mo may have negative effect on material as they facilitate the formation of intermetallic phases at high temperatures, these elements will also assist to increase toughness value if

the welding parameters are controlled to avoid formation of intermetallic phases. In otherwords, it is understood that the SDSS materials are more prone for sigma and secondary austenite phase formation than DSS samples, which may lead to loss of toughness in SDSS weldments, if the welding parameters are not controlled properly. Figure 4.17 (a) and (b) shows SEM images of the fractured surfaces of the DSS and SDSS joints.

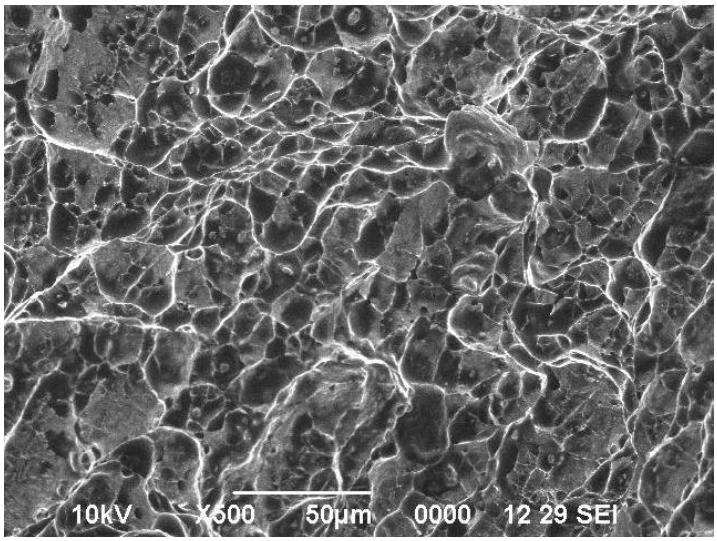

a) DSS

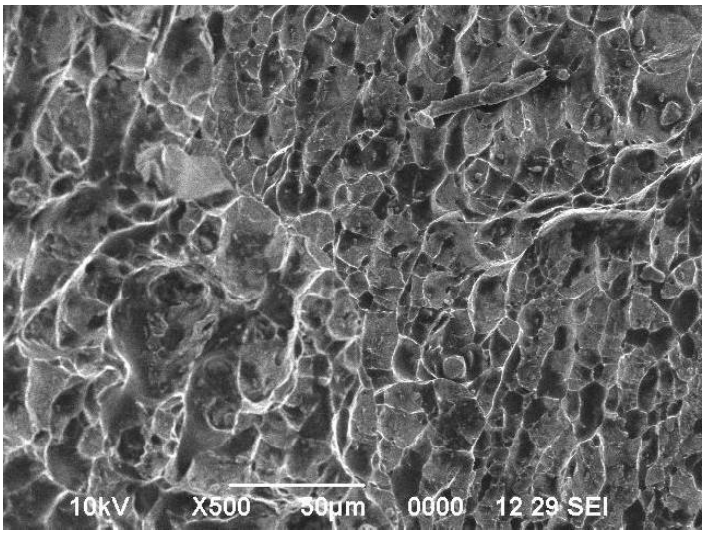

b) SDSS

Figure 4.17: SEM images of fractured samples during Charpy V-notch impact test

It can be seen that both materials show sign of ductile fracture as dimples are observed. Fractography for DSS / SDSS specimen exhibit more dimples and smaller average dimple size which suggests ductile mode of facture is dominant in fractured welded samples [126]. Cleavages (i.e. flat surafces) are also observed in both specimen which indicates minor brittleness of the joint.

The impact toughness varies from weld center, HAZ and fusion line as the microstructure of these locations are different. Thus, we have selected different location to study the impact toughness properties. As recommended by many offshore standards, study was conducted by creating a V-notch at four different locations, which are (1) weld metal, (2) fusion line, (3) 2 mm from fusion line and

(4) 5 mm from fusion line. Figure 4.18 shows the impact toughness values with respect to four different V-notch locations.

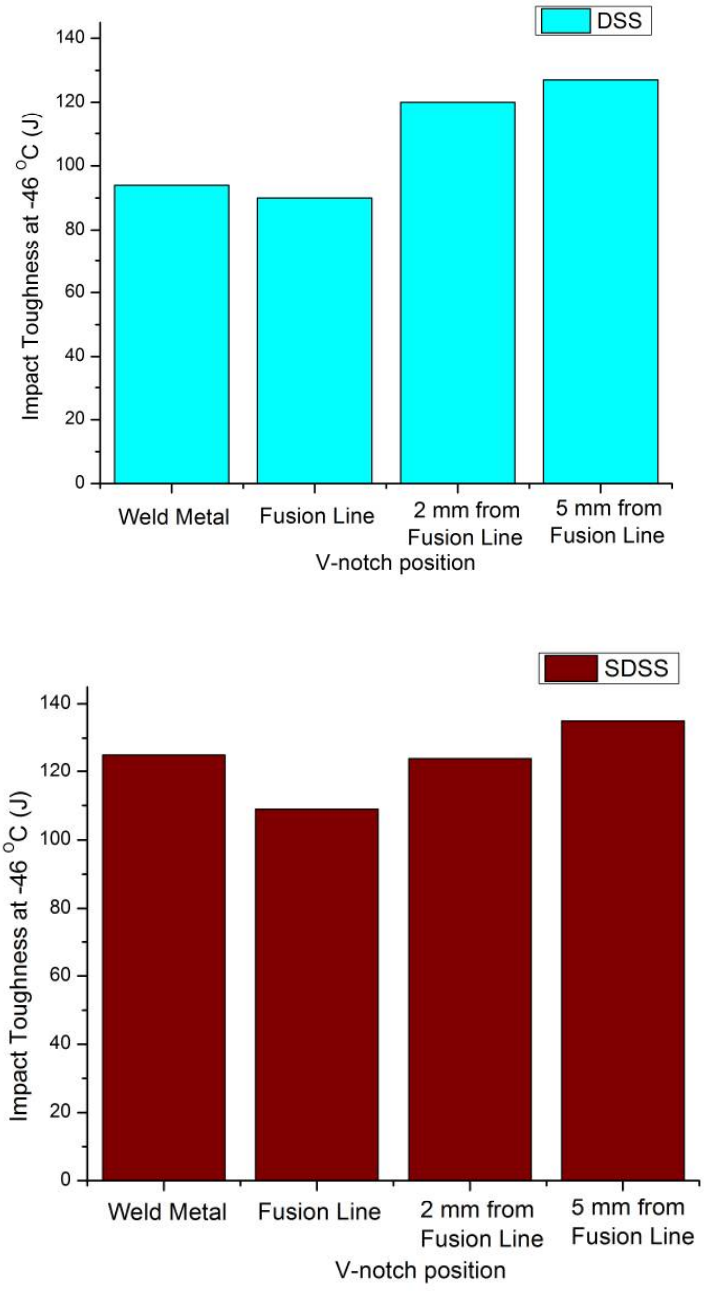

Figure 4.18: Impact toughness values at different V-notch positions

Low impact toughness values are observed at weld metal and further lower impact toughness values are obtained in fusion line as compared to weld center. This is because solidification starts at the fusion line interface, which reduces the impact toughness value.

Higher Impact toughness values are observed at V-notch positions at 2 mm and 5 mm from fusion line when compared with weld center. Increased toughness values are noted because, the V notch was made in base metal (2mm and 5mm from fusion line), the microstructure and alloying elements are not largely affected by welding filler wire on these locations and the only factor influenced is heat input. Impact toughness properties of both DSS and SDSS joints are considerably improved when higher nitrogen content gas mixture is used as shielding and purging gas. Increase in nitrogen content will broaden separation between two dislocation planes, which restricts the dislocations to their own slip planes [164], thus facilitates improved toughness properties.

An increase in inter-pass temperature has a negative effect on impact toughness value because of prolonged exposure to sensitive temperature range, which causes formation of sigma phases / secondary austenite in weld zone. This brittle sigma phase is the main reason for the loss of toughness values in weldments.

4.4 PITTING CORROSION TEST

4.4.1 ASTM G48 test

The pitting corrosion test results are tabulated in Table 4.7 and 4.8.

Table 4.7- Corrosion test results for DSS weldments

Exp No.	Specimen	Heat Input (kJ/mm)	Corrosion rate g /(m^2 / day) at 22 ^{O}C	Corrosion rate g /(m^2 / day) at 28 ^{O}C
1	DSS- Low PREN	1.05	0.250	2.65
2		1.1	0.311	3.95
3		1.15	0.40	6.11
4		1.2	0.591	7.63
5	DSS- High PREN	1	0.099	1.96
6		1.05	0.103	2.39
7		1.1	0.111	3.45
8		1.15	0.559	4.65

Table 4.8- Corrosion test results for SDSS

Exp No.	Specimen	Heat Input (kJ/mm)	Corrosion rate g /(m^2 / day) at 35 ^{O}C	Corrosion rate g /(m^2 / day) at 40 ^{O}C
1	SDSS- Low PREN	0.95	0.127	1.148
2		1.05	0.139	2.046
3		1.15	0.198	2.731

4		1.25	0.246	4.842
5	SDSS-High PREN	0.75	0.091	1.391
6		1	0.103	1.928
7		1.1	0.178	2.364
8		1.2	0.236	3.687

The variation of corrosion rate with respect to heat input is shown in Figure 4.19 (a) and (b).

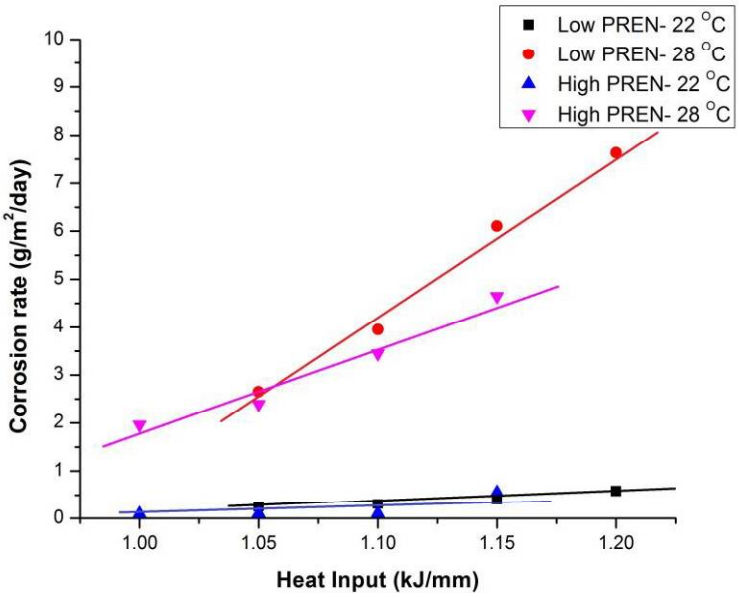

a) DSS weldments

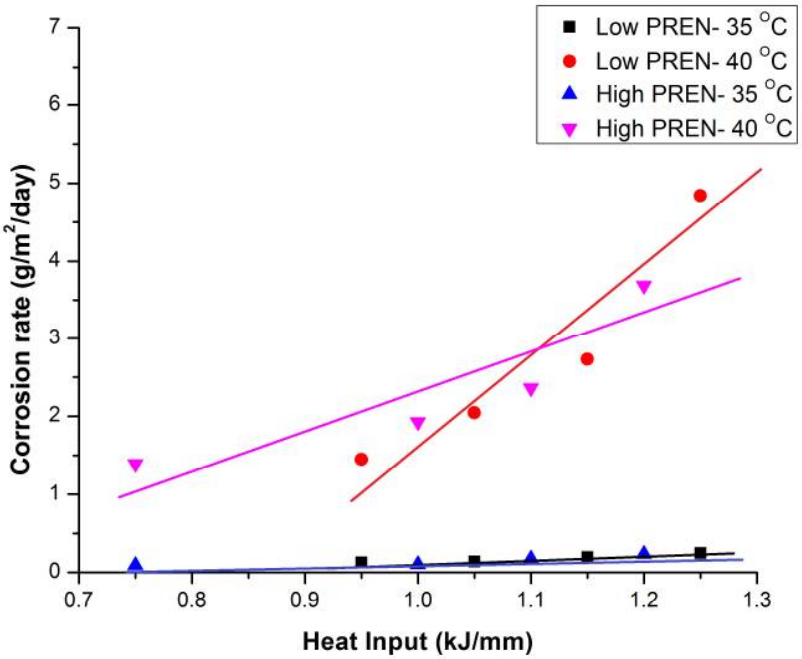

b) SDSS weldments

Figure 4.19: Variation of corrosion rate with heat input

It can be seen from Figure 4.19 that the corrosion rate is found to be increasing with the increase in the heat input. This could be because, at high heat input the weld region attains sensitive temperature range where formation of intermetallics phases such as sigma pahse and secondary austenite takes place easily. The secondary austenite contains very low amount of Cr and Mo. Hence, these sites are the sites for pitting corrosion attack due to easy breakdown of the passive film. For DSS, at 22 ºC, there is no evidence of pitting, i.e. (weight loss < 1 g /m^2 in 24 hours). However, when the temperature is increased to 28 ºC, pits are observed on the weldments. According to ASTM G48 test, the stable pitting is said to be

initiated when weight loss is more than 1 g /(m^2.day). On all the DSS samples, pits are observed at 28 ºC. Similarly, for SDSS weldments, a weight loss of more than 1 g /(m^2.day) is observed on all samples at 40 ºC.

Corrosion rate against heat input in the form of bar charts is shown in Figure 4.20.

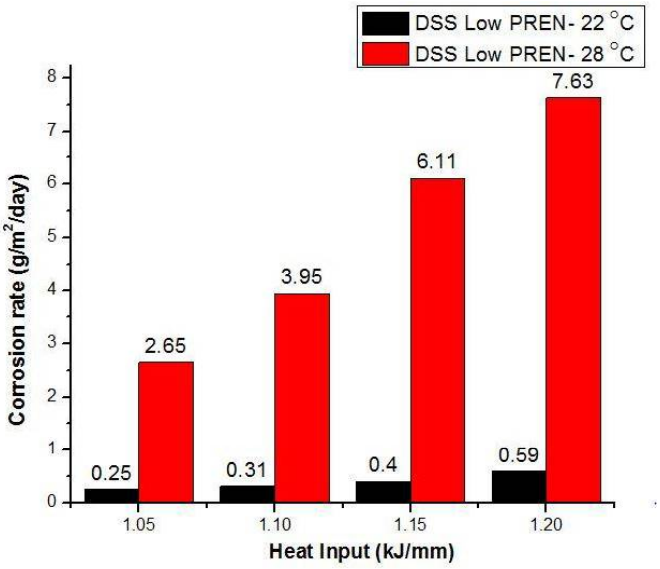

a) DSS- Low PREN

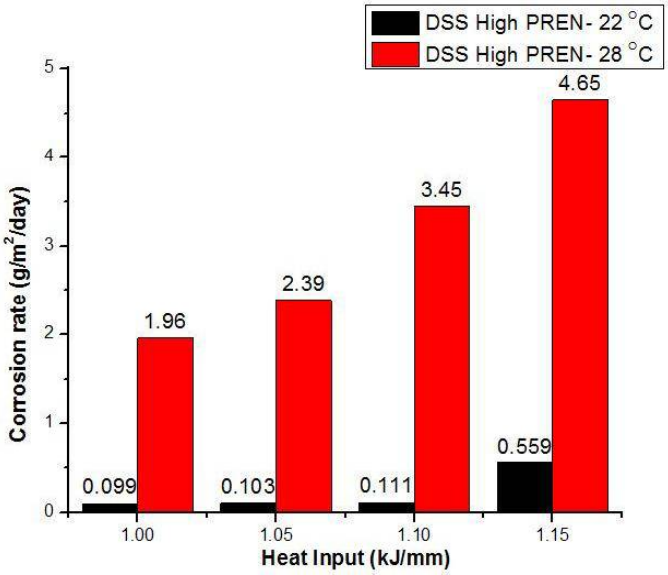

b) DSS- High PREN

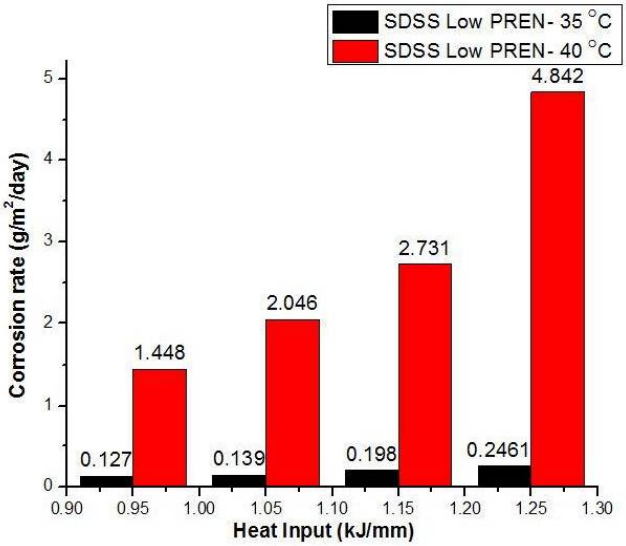

c) SDSS- Low PREN

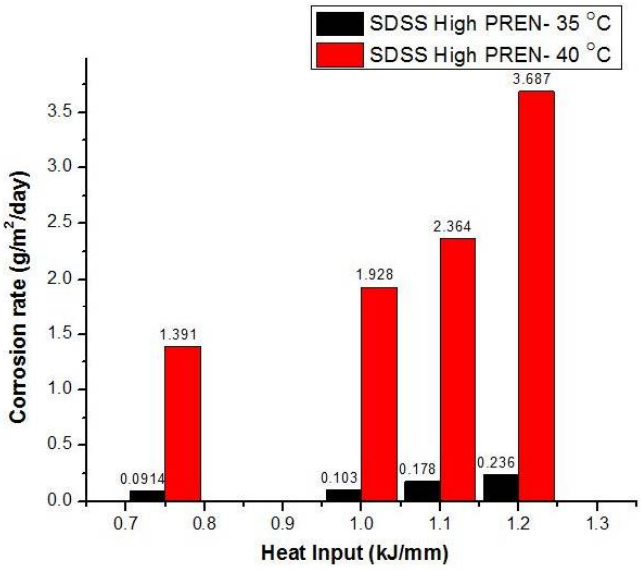

d) SDSS- High PREN

Figure 4.20: ASTM G48 Corrosion test results

Typical samples after ASTM G48 tests are shown in Figure 4.21.

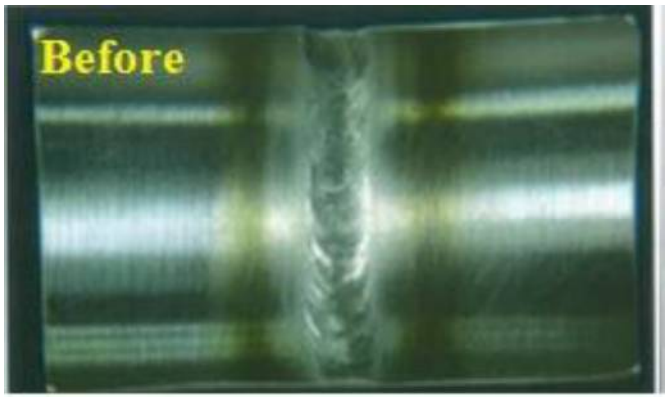

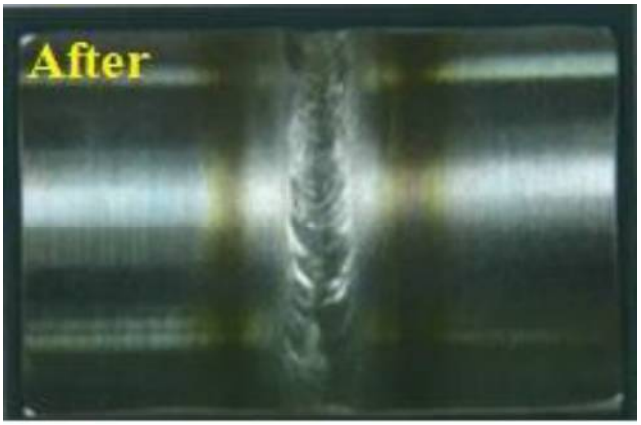

a) DSS weldments

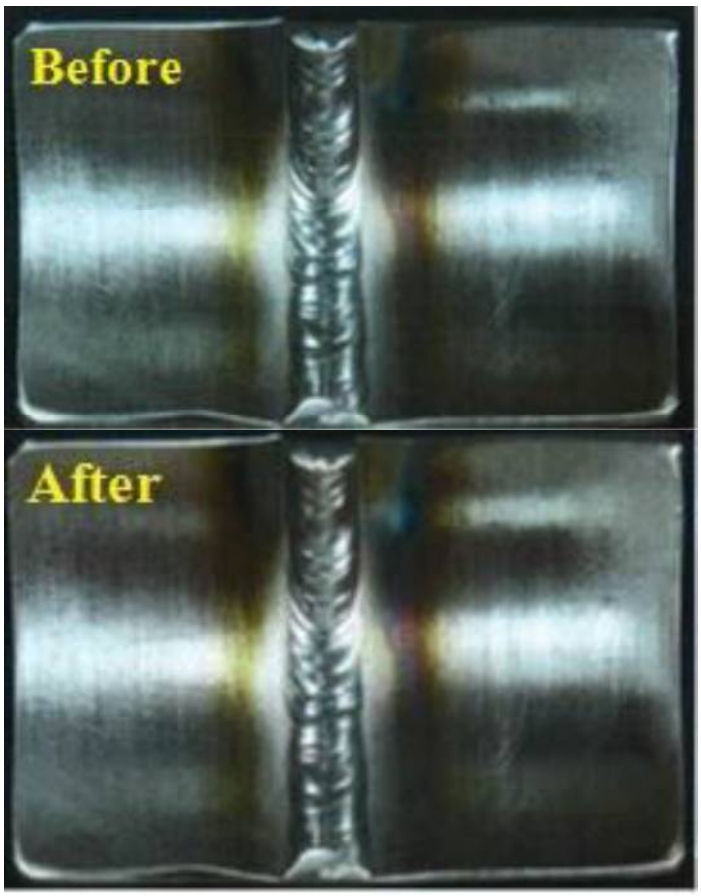

b) SDSS weldments

Figure 4.21: Typical specimen before and after ASTM G48 test

In the second part, the shielding/purging gas and the inter-pass temperatures were varied as detailed in Table 3.5 and Table 3.6. The results of the tests are tabulated in Table 4.9 and Table 4.10.

Table 4.9- Effect of shielding/purging gas and inter-pass temperature on Corrosion test results for DSS weldments

Exp. No.	Heat Input (kJ/mm)	Corrosion rate g /(m^2 / day) at 22 ^{O}C	Corrosion rate g /(m^2 / day) at 28 ^{O}C
1 (Ar+2%N_2, 120 ^{O}C)	1.05	0.25	2.65
2 (Ar+5%N_2, 120 ^{O}C)	1.05	0.124	1.64
3 (Ar+2%N_2, 160 ^{O}C)	1.05	0.179	1.68
4 (Ar+2%N_2, 160 ^{O}C)	1.05	0.768	4.49

Table 4.10- Effect of shielding/purging gas and inter-pass temperature on Corrosion test results for SDSS weldments

Exp. No.	Heat Input (kJ/mm)	Corrosion rate g /(m^2 / day) at 35 ^{O}C	Corrosion rate g /(m^2 / day) at 40 ^{O}C
1 (Ar+2%N_2, 120 ^{O}C)	0.95	0.127	1.148
2 (Ar+5%N_2, 120 ^{O}C)	0.95	0.0968	0.945
3 (Ar+2%N_2, 160 ^{O}C)	0.95	0.0984	0.958
4 (Ar+2%N_2, 160 ^{O}C)	0.95	0.678	5.92

It is found that addition of more nitrogen in the shielding / backing gas mixtures has positive effects on corrosion properties due to austenite and ferrite phase balance. Pitting resistance of individual phases are also improved due to proper

partitioning of elements [163]. The increase in inter-pass temperature increases pitting corrosion rate, as noticed by the weight loss results.

4.4.2 Potentiodynamic polarization tests

The results of potentiodynamic polarization tests for best and worst corrosion behavior of both DSS and SDSS are shown in Figure 4.22 (a) and (b). It can be seen that potentials shift to more positive values for specimen at low heat input.

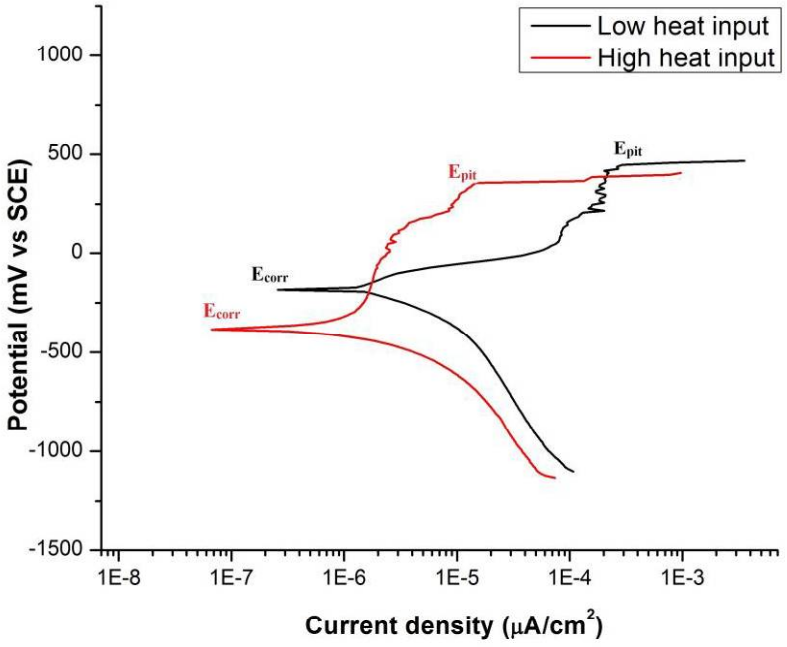

a) DSS

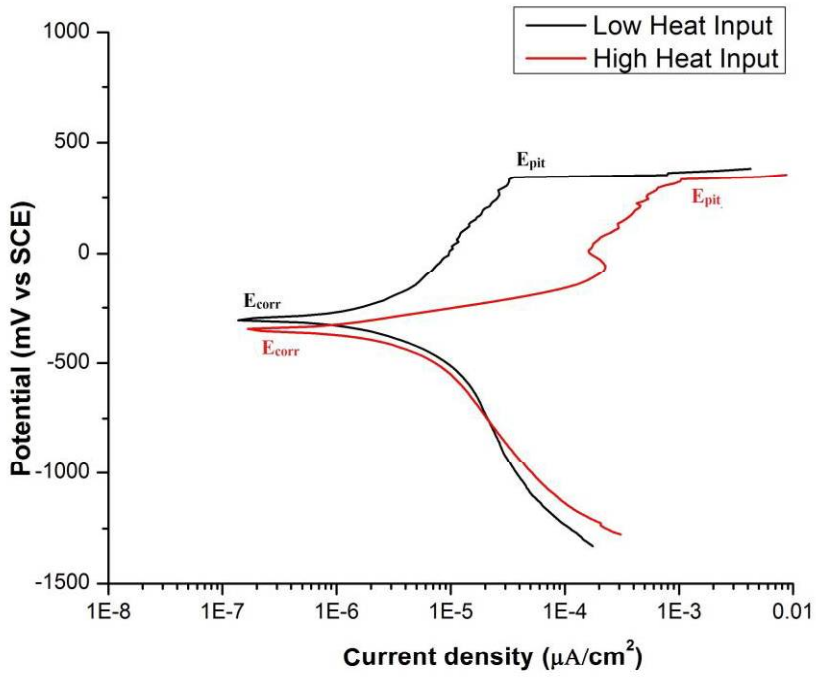

b) SDSS

Figure 4.22: Polarization curves for DSS and SDSS Material

The corrosion potential (E_{corr}) and pitting potential (E_{pit}) for DSS and SDSS speciemens are tabulated in Table 4.11.

Table 4.11- Effect of Heat input on Corrosion and pitting potentials for DSS and SDSS (mV SCE)

Specimen	E_{pit}	E_{corr}	E_{pit}-E_{corr}
Low heat input- DSS	467	-189	656
High heat input-DSS	406	-216	622
Low heat input- SDSS	382	-321	703
High heat input-SDSS	353	-347	700

The difference between them i.e. (E_{pit} - E_{corr}) is a measure of resistivity of passive film on the specimen. The larger the difference, better is the corrosion resistance [144]. The least corrosion resistance is observed for few samples due to the formation of secondary austenite and improper partitioning of individual phases.

The typical corroded specimen analyzed through SEM are shown in Figure 4.23 (a0 and (b).

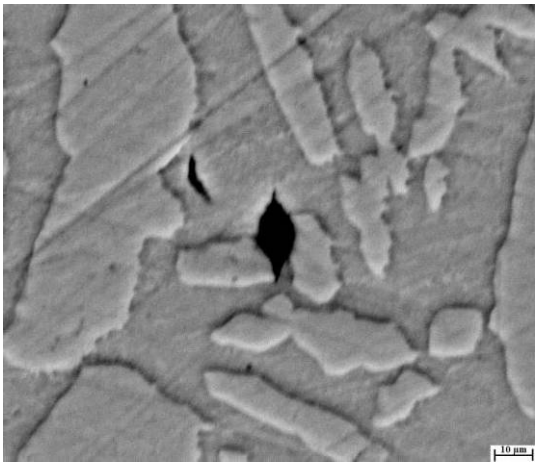

a) DSS

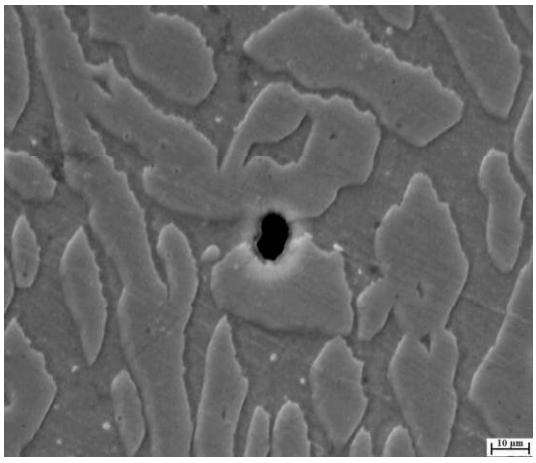

b) SDSS

Figure 4.23: Typical SEM images of corroded specimen

The results of second part of the studies which is the effect of shielding gas / purging gas and interpass temperature are tabulated in Table 4.12 and Table 4.13.

Table 4.12- Effect of Shielding / purging gas and inter-pass temperature on Corrosion and pitting potentials of DSS weldments (mV SCE)

Specimen	E_{pit}	E_{corr}	E_{pit}-E_{corr}
1 (Ar+2%N_2, 120 ^{O}C)	434	-164	598
2 (Ar+5%N_2, 120 ^{O}C)	472	-149	621
3 (Ar+2%N_2, 160 ^{O}C)	484	-143	627
4 (Ar+2%N_2, 160 ^{O}C)	335	-215	550

Table 4.13- Effect of Shielding / purging gas and inter-pass temperature on Corrosion and pitting potentials of SDSS weldments (mV SCE)

Specimen	E_{pit}	E_{corr}	E_{pit}-E_{corr}
1 (Ar+2%N_2, 120 ^{O}C)	392	-418	810
2 (Ar+5%N_2, 120 ^{O}C)	430	-367	797
3 (Ar+2%N_2, 160 ^{O}C)	445	-328	773
4 (Ar+2%N_2, 160 ^{O}C)	375	-336	711

It is clear that the addition of nitrogen in shielding and back purging gas increases pitting nucleation resistance. When the interpass temperature is increased, both corrosion potential (E_{corr}) and pitting potential (E_{pit}) shift to negative side which results in decrase of corrosion resistance.

4.4.3 Critical Pitting Temperature measurements

CPT measuremenrs are carried out by potentiostatic measurements to confirm maximum working temperatures for weldments. The CPT is the temperature at which corrosion current density reaches 100 µA/cm^2. It is found that in all DSS weldments, stable pitting occurrs in between 23 ºC to 27 ºC. For SDSS, it is found to be in between 37 ºC to 41 ºC as shown in Figure 4.24.

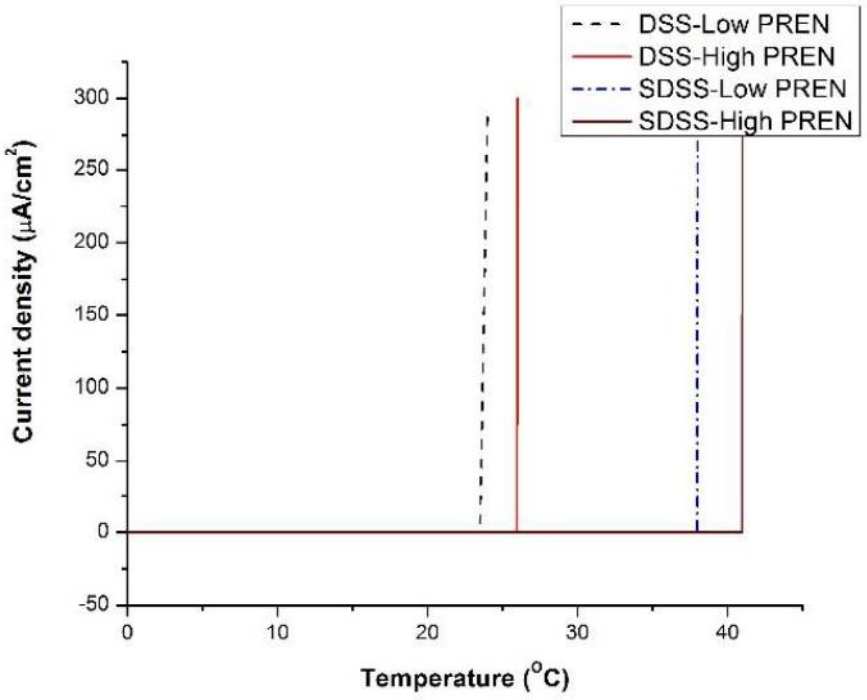

Figure 4.24: Critical pitting temperature measurements

4.4.4 PREN of individual phases

PREN of ferrite and austenite phases are studied to understand cause and the area of pitting attack region as tabulated in Table 4.14.

Table 4.14- Alloying element contents (% wt.) and PREN of individual phases

Specimen	Phase	Cr	Mo	Ni	N	PREN
DSS-Highest corrosion rate	α	22.30	3.32	7.87	0.05	34.05
	γ	21.93	2.81	7.96	0.22	34.72
	γ_2	11.52	0.90	8.10	0.20	17.69
DSS-Lowest corrosion rate	α	24.12	3.24	7.35	0.05	35.61
	γ	21.70	2.74	7.81	0.27	35.06
	γ_2	12.86	0.96	8.12	0.23	19.70
SDSS Highest corrosion rate	α	25.24	3.82	8.52	0.05	38.64
	γ	23.12	3.52	8.82	0.39	40.97
	γ_2	14.08	1.11	8.76	0.32	22.86
SDSS-Lowest corrosion rate	α	25.15	3.92	8.52	0.05	38.88
	γ	23.46	3.64	8.72	0.35	41.07
	γ_2	14.24	1.23	8.74	0.31	23.25

The elemental composition of each phase is observed through SEM-EDS. The typical EDS study is shown in Figure 4.25.

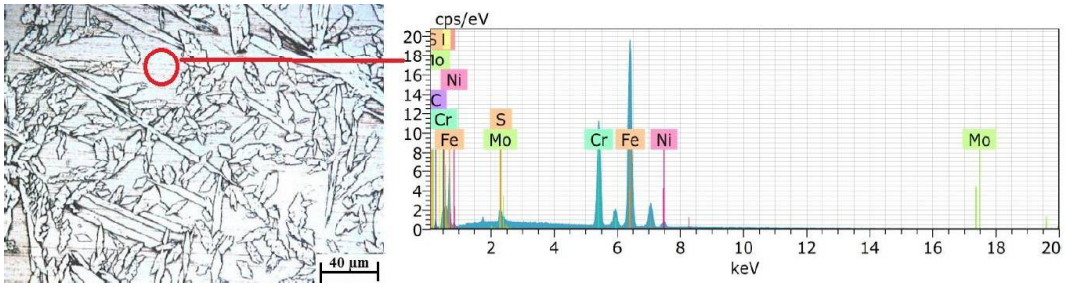

Figure 4.25: EDS study of the welded samples

The pitting resistance equivalent number is calculated by formula: PREN= % Cr + 3.3 % Mo + 16 % N. Due to different elemental partitioning, each phase is having different PREN value. However, due to rapid cooling cycles, the partitioning ratio tends to unify for Cr, Mo and Ni. In case of nitrogen, it is assumed that ferrite reaches its saturation level of 0.05 %. The rest is partitioned in austenite phase. Hence, the nitrogen content in the austenite phase can be calculated on the basis of the content of nitrogen in the whole alloy and the phase volume fraction. The new austenite phase is found to have reduced Cr content and very low Mo content. Similar observations are made in other literatures [101]. It is understood that the pitting attack occurs in secondary austenite phase region.